JOURNAL OF MATERIALS SCIENCE 13 (1978) 27–36

Hydrogen bubbles in embrittled Al-Zn-Mg alloys

G. M. SCAMANS
Alcan Laboratories Limited, Southam Road, Banbury, Oxon, UK

Al–Zn–Mg alloys become embrittled during exposure to moist environments due to hydrogen penetration of grain boundaries. The result of this hydrogen penetration due to surface reaction with water vapour of both bulk specimens and electron-transparent "thin foils", has been studied at high resolution in the JEM 100 C transmission electron microscope as a function of alloy composition and ageing treatment. In bulk specimens of alloys solution-heated, water-quenched, and aged in water-vapour-saturated air at 70° C, the hydrogen is in the form of a mobile atomic species which is transformed to bubbles of molecular hydrogen under the action of the electron beam. However, in electron-transparent specimens of aged alloys after exposure to water vapour the accumulated hydrogen is observed directly as bubbles. These bubbles take the form of hexagonal lenses bounded by {1 1 1} planes, and are associated with grain-boundary precipitates, particularly in over-aged microstructures, and with primary intermetallic particles in alloys containing sparingly soluble transition elements. The consequence of the observed hydrogen penetration of grain boundaries in promoting environmental debilitation of mechanical properties and stress-corrosion cracking of Al–Zn–Mg alloys is discussed.

1. Introduction

The degradation of mechanical properties of tensile specimens of Al–Zn–Mg [1, 2] alloys during exposure to water vapour has been ascribed to hydrogen penetration of grain boundaries. This role of hydrogen has been supported by the following critical observations:

(1) The wholly brittle nature of the intergranular fracture at the highest resolution studied in the high voltage electron microscope (HVEM) [1].

(2) The coincidence ot the fracture path with the grain boundary plane [1].

(3) The detection of hydrogen evolution during elastic stressing of embrittled tensile specimens in vacuum together with a full recovery of ductility [2].

(4) The direct observation of bubbles of molecular hygrogen on grain boundaries [3, 4].

(5) The measurement of high rates of hydrogen penetration of Al–Zn–Mg alloys as compared to pure aluminium [5].

(6) The measured accumulation of a high concentration of hydrogen beneath surface films of embrittled specimens [6].

In the present study, which is part of a general investigation of environmentally sensitive mechanical behaviour of Al–Zn–Mg alloys, the JEM 100 C high-resolution transmission electron microscope has been used to examine the effect of hydrogen penetration on grain-boundary morphology as a function of alloy composition, pre-exposure environment, heat treatment and specimen thickness. Various alloying elements were added for different reasons. The iron and silicon additions, nominally 0.10 and 0.05 wt% respectively, are levels that can normally be expected in high-purity commercial material. It was considered that the additions of Cr, Mn and Zr (nominally 0.10, 0.30 and 0.14 wt% respectively) would be more relevant in terms of grain refinement characteristics and intermetallic phase composition in the presence of iron and silicon. The object of making these additions was to study

TABLE I Compositional analyses of alloys

Alloy No.	Fe %	Mg %	Si %	Ti %	Zn %	B ppm	Others %
1	< 0.01	1.5	< 0.01	0.010	4.30	12	
2	0.11	1.53	< 0.01	0.010	4.45	9	
3	< 0.01	1.52	0.05	0.010	4.43	9	
4	0.11	1.52	0.05	0.012	4.42	12	
5	0.10	1.54	0.05	0.010	4.45	12	Cr 0.10
6	0.11	1.56	0.05	0.011	4.40	12	Mn 0.33
7	0.11	1.56	0.06	0.011	4.50	10	Zr 0.14

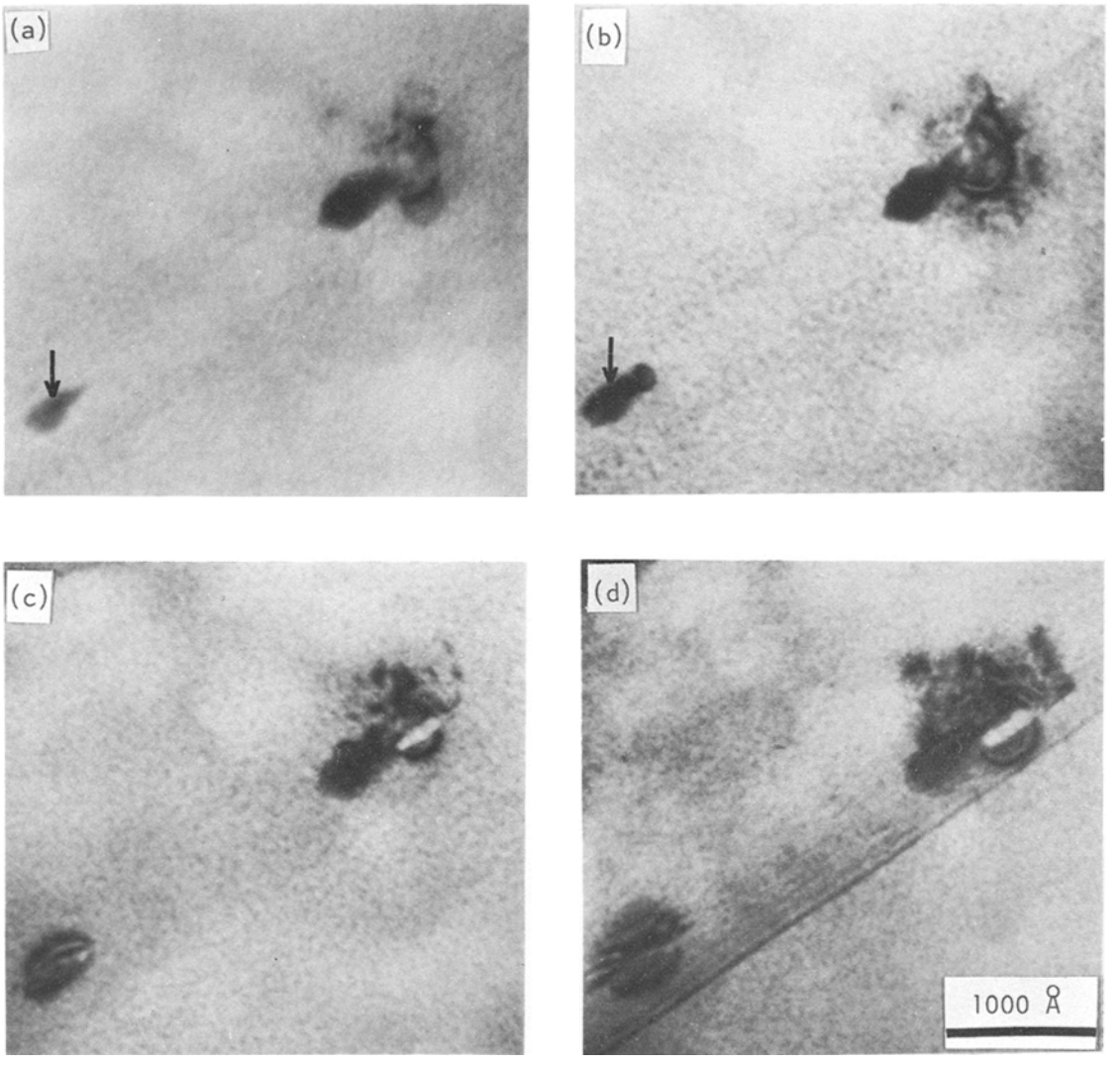

Figure 1 Dynamic sequence showing the interaction of 120 kV electron beam with the accumulated grain-boundary hydrogen after 70 days exposure to WVSA at 70° C before thin foil preparation (Alloy 1). (a) After 10 sec (BF $g = 2\,0\,0, s \neq 0$). (b) After 10 min (Note the bubble nucleation at the second grain-boundary precipitate (arrowed). (c) After 30 min. (d) After 35 min (BF $g = 2\,0\,0$, s + ve) (Note the high local dislocation density.)

the role of primary intermetallic particles situated at grain boundaries on the directly observed effects of hydrogen penetration.

2. Experimental

The compositional analyses of the d.c. cast ingots used in this study are shown in Table I.

The scalped ingots (cross-section 200 mm × 65 mm) were homogenized for 16 h at 465° C followed by hot-rolling to 5 mm. After an intermediate anneal a final sheet thickness of 0.5 mm was obtained by cold-rolling. Specimen coupons (45 mm × 10 mm) were cut from the rolled sheet of the base alloy (Alloy 1) and given a standard solution heat-treatment of 30 min at 465° C in air, followed by cold-water quenching and chemical polishing in Phosbrite 159. The coupons were then left either at 0% or 100% Relative Humidy (r.h.) at 70° C for up to 96 days. Thin foil specimens were then prepared from the pre-exposed coupons in order to examine the effect of hydrogen penetration of "bulk" specimens on grain-boundary morphology.

Hydrogen accumulation in electron-transparent specimens was examined in all the alloys in thin foils prepared both from as-quenched and artificially aged material. The ageing treatments used after water quenching were 48 h at room temperature followed by 4 h at 90° C and either 4 h at 150° C or 7 days at 150° C. The first treatment, which is less than peak ageing, would make the alloy highly stress-corrosion susceptible. The second treatment imparts a degree of over-ageing and an increase in stress-corrosion resistance. Thin foil specimens of as-quenched and aged alloy were exposed both to laboratory air at room temperature and to water-vapour-saturated air at 70° C prior to examination at 120 kV in the electron microscope.

3. Results

3.1. Hydrogen accumulation in 0.5 mm thick specimen coupons during pre-exposure to water-vapour-saturated air at 70° C

These observations were made on thin foil specimens prepared from 0.5 mm thick coupons of the base alloy which had been exposed at 70° C either to water-vapour-saturated air (WVSA) or to dry air. Electron microscope specimens were examined as soon as possible, i.e. within a few minutes of having been electro-polished. Thin foils prepared from specimens exposed to dry air showed no unexpected features whereas those prepared from specimens exposed to WVSA showed direct evidence of grain-boundary penetration by hydrogen. This is shown in Fig. 1, which shows a dynamic sequence of the interaction of the electron beam with the accumulated grain-boundary hydrogen. The SHT and WQ coupon of the base alloy was pre-exposed to WVSA for 70 days at 70° C. Fig. 1a shows the immediate transformation of the accumulated grain-boundary hydrogen to form a bubble visible by strain field contrast in the bright field (BF) image in the vicinity of a grain-boundary precipitate. This occurred within a few seconds of the beam being positioned in this area and it should be noted that at this time there is no bubble associated with the second grain-boundary precipitate (arrowed). After 10 min beam heating, the same area, under the same kinematical diffracting conditions, is shown in Fig. 1b. The second grain-boundary precipitate has now nucleated a hydrogen bubble, again revealed by strain field contrast, and there has been considerable dislocation activity in the region of the larger precipitate as can be seen in Fig. 1c which again shows the same area after 25 min exposure to the beam. Eventually a void of projected dimensions 450 Å × 100 Å has developed at the first precipitate (Fig. 1d). The image in Fig. 1d was recorded with a reduced value of the deviation parameter s, i.e. under more dynamical conditions, in order to increase the contrast of the generated dislocations ($g = 200\ s + ve$)*. By positioning the electron beam in previoulsy non-irradiated regions of the thin foil specimen events similar to those depicted in Fig. 1 could be readily promoted.

It should be emphasized that the effects described above occurred only in foils of bulk specimens that had been exposed to water vapour. Severe irradiation of thin foil specimens of alloys exposed to dry air produced only grain-boundary precipitate coarsening due to electron beam heating. Exposure of bulk specimen coupons of alloys of this type to WVSA at 70° C produces both a reduction in elongation and a loss of tensile strength together with the appearance of fully brittle inter-granular fracture facets [2].

*The notation s + ve requires that the BF image has been recorded under two-beam dynamical conditions with a small positive deviation from the Bragg position in order the enhance transmission and contrast.

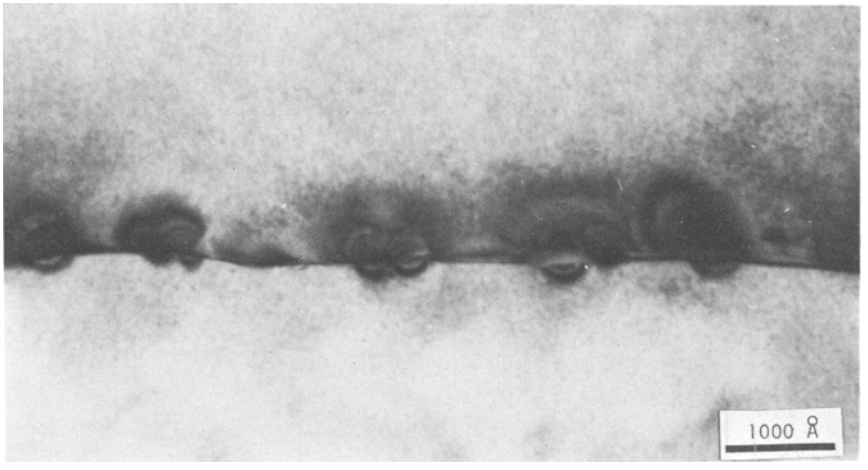

Figure 2 Hydrogen bubble formation on a grain boundary (Alloy 1) of a thin foil specimen during exposure to laboratory air after 96 days ageing at 70° C and 0% r. h. (BF $\mathbf{g} = 2\,2\,0, s$ + ve upper grain and $\mathbf{g} = 1\,1\,1, s$ + ve lower grain.)

3.2. Hydrogen accumulation in thin foil material

It was first suspected that thin foil specimens of Al–Zn–Mg alloys would readily accumulate hydrogen during storage in laboratory air when, on examination in the electron microscope, specimens prepared from bulk specimens pre-exposed to dry air at 70° C, i.e. non-embrittled specimens, were observed to have hydrogen bubbles on grain boundaries. However, such bubbles were not observed, as reported in Section 3.1, in freshly prepared specimens. A typical example of this effect is shown in Fig. 2. The bulk specimen was exposed for 96 days at 70° C and 0% r.h. before thin foil preparation, and the thin foil was exposed for 14 days in laboratory air at room temperature before examination in the microscope. Clearly, hydrogen penetration of the thin foil specimen has produced a high density of bubbles on the imaged grain-boundary.

The image widths of the strain fields of the hydrogen bubbles vary across the grain-boundary due to the change in operating reflection. The line of no contrast tends to lie in the grain-boundary plane rather than perpendicular to the operating reflection. The strain field image widths in each grain are of the order of half the extinction distance for the particular operating reflection as would be expected for dynamical Ashby–Brown type strain field images [7]. This observation that thin foil material would rapidly show effects of hydrogen penetration proved a convenient method to study compositional, ageing and environmental effects on hydrogen accumulation.

3.3. Effect of alloy composition and heat treatment on hydrogen accumulation in thin foil specimens under ambient conditions

3.3.1. As-quenched

Immediate examination and subsequent examination after 3 months storage in laboratory air at room temperature revealed no evidence of hydrogen accumulation in any of the alloys examined. In all cases the grain boundaries were completely free of $MgZn_2$ precipitates and the matrix precipitates consisted of fine spherical GP zones 5 to 10 Å in diameter.

3.3.2. Artificially aged

The accumulation of hydrogen in thin foil specimens of artificially aged alloys (48 h at room temperature + 4 h at 90° C + 4 h at 150° C) during three months exposure to laboratory air at room temperature is shown in Figs. 3 and 4. There was no obvious distinction between the observed bubble morphology for any of the artificially aged alloys examined. Bubble density varied considerably from one grain-boundary to another and even along individual boundaries, making quantitative analysis impossible. An example of grain-boundary hydrogen bubbles in an artificially aged alloy (Alloy 4) is shown in Fig. 3a and b. The images were recorded under different operating reflections, $\mathbf{g} = 2\,2\,0$ and $\mathbf{g} = 2\,0\,0$ respectively.

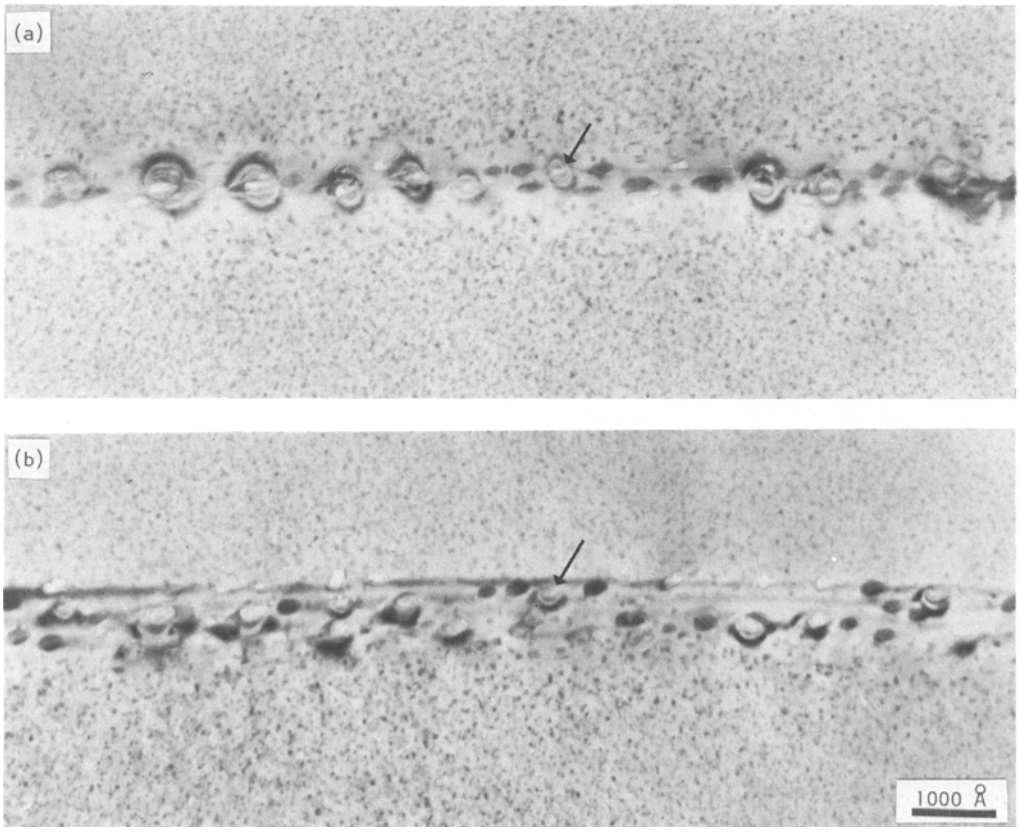

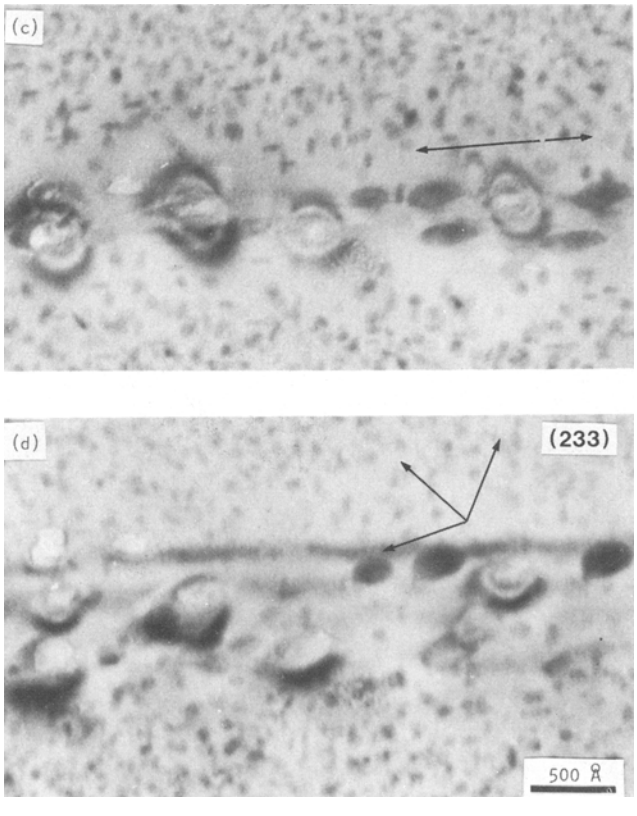

Figure 3 Hydrogen bubble development during three months exposure of a thin foil specimen of an artificially aged alloy (Alloy 4) to laboratory air. (a) BF $\mathbf{g} = 2\,2\,0$ s + ve. (b) BF $\mathbf{g} = 2\,2\,0$ s + ve. (c) close-up of (a). (d) close-up of (b) showing traces of $\{1\,1\,1\}$ planes. (Note the changes in bubble shape on tilting.)

There is some association of the hydrogen bubbles with the grain-boundary $MgZn_2$ precipitates although some bubble nucleation has occurred directly on the grain-boundary plane (as arrowed in Fig. 3a and b). Regions where precipitates have been "leached out" during polishing show no strain field contrast and hence can be readily distinguished. The projected shape of the bubble changes on tilting of the thin foil specimen as can be seen from a comparison of Fig. 3a and 3b and this change of shape is, to some extent, mirrored by the change in grain-boundary precipitate shape. This is shown at higher magnification in Fig. 3c and d. In Fig. 3c it can be seen that the trace direction of the bubble wall is parallel to a matrix precipitate habit plane and that this particular precipitate variant occurs in both of the grains. The habit plane for the precipitate which has been termed η' has been determined to be $\{1\,1\,1\}$ [8]. On tilting (Fig. 3d) the observed shape of the bubble changes to an irregular hexagon. All the bubbles on the boundary present similar projected aspects, the principal trace directions of which are shown on the micrograph. These directions are consistent with traces of $\{1\,1\,1\}$ planes in the upper grain which has a (2 3 3) orientation as determined by selected area diffraction. This type of bubble morphology was observed in all the alloys studied, the plane of the lens-shaped bubble usually being coincident with the grain-boundary plane. Hexagonal bubble sections were most frequently observed although in some cases they were square or triangular. In all cases where trace analysis was possible, the bubble walls were consistent with $\{1\,1\,1\}$ matrix planes.

A second example of hydrogen bubbles in an aged alloy (Alloy No. 7) is shown in Figs. 4a to c.

Figure 4 Variation in hydrogen bubble contrast on tilting (Alloy 7) after similar thin foil exposure as in Fig. 3. (a) BF $g = 1\,1\,1, s \neq 0$ (b) BF $g = 4\,4\,4, s = 0$ (c) BF $g = 2\,2\,0, s$ + ve.

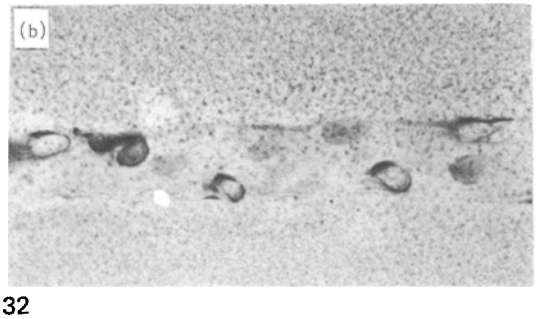

In Fig. 4a under a weakly excited bright field kinematical condition the bubbles have effectively vanished. The bubbles, however, become visible using a fourth order low-index reflection as shown on Fig. 4b ($g = 4\,4\,4$). The bubble morphology can be most readily appreciated under these reflecting conditions where the strain field contrast is minimized consistent with retaining bubble visibility. Fig. 4c shows the same area imaged using a more strongly excited dynamical reflection condition ($g = 2\,2\,2\,s$ + ve)

The association of the grain-boundary hydrogen bubbles with the $MgZn_2$ grain-boundary precipitate is not strong in the peak-aged alloys. However, primary intermetallic particles such as occur, for example, in the alloys containing additions of transition elements, show a distinct propensity for promoting bubble nucleation as is shown in Fig. 5 for the manganese-containing alloy (Alloy 6). A single bubble has developed at a hexagonal manganese-rich particle. These particles may therefore exert a local gettering effect on the grain-boundary hydrogen.

The effect of increased ageing time at 150° C is shown in the bright field image in Fig. 6 (Alloy 1) under dynamical reflecting conditions ($g = 2\,0\,0\,s$ + ve). The hydrogen bubbles show a greater affinity for the larger $MgZn_2$ grain-boundary precipitates. The study of precipitate/bubble interactions in overaged microstructures is however difficult in thin foil specimens which are electron-

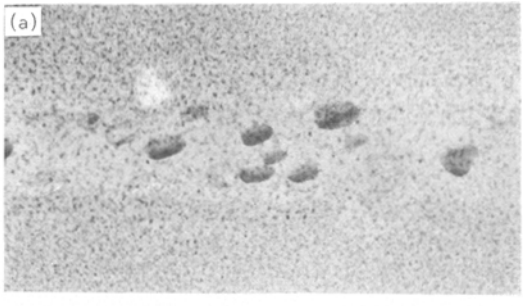

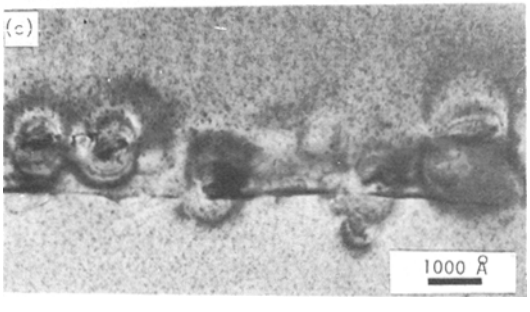

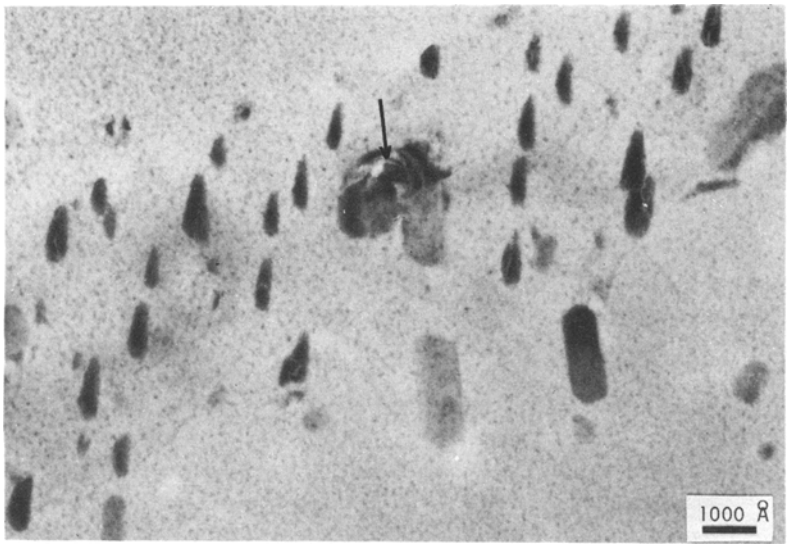

Figure 5 Preferential hydrogen bubble nucleation on a manganese-rich grain-boundary intermetallic phase (Alloy 6).

transparent at 120 kV as the precipitate particle width approximates to the foil thickness. A study of this type is greatly facilitated by use of the high-voltage electron microscope [3].

3.4. Exposure of thin foil specimens to water-vapour-saturated air at 70° C

3.4.1. As-quenched

The effect of exposure to WVSA at 70° C of a freshly prepared specimen in the solution-treated and water-quenched condition is shown in Fig. 7. Fig. 7 is of the base alloy exposed to the environment for 3 h prior to examination in the electron microscope. The micrograph shows the preferential location of pseudo-boehmite islands (identified by selected area electron diffraction) along grain-boundary/surface intersections. As a result of a few seconds of beam irradiation, hydrogen bubbles form on the grain-boundaries and then gradually disappear. The imaged grain-boundary shows both newly formed bubbles exhibiting strong strain field contrast and disappearing bubbles showing weak strain field contrast. In some cases bubbles also appeared very briefly within the grains near

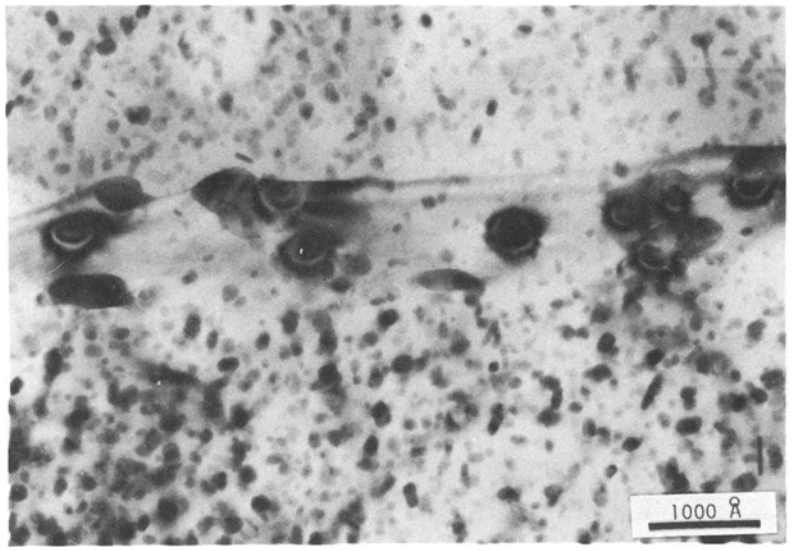

Figure 6 Association of the hydrogen bubbles with the equilibrium grain-boundary precipitates in an overaged microstructure (Alloy 1) BF g = 2 0 0, s + ve.

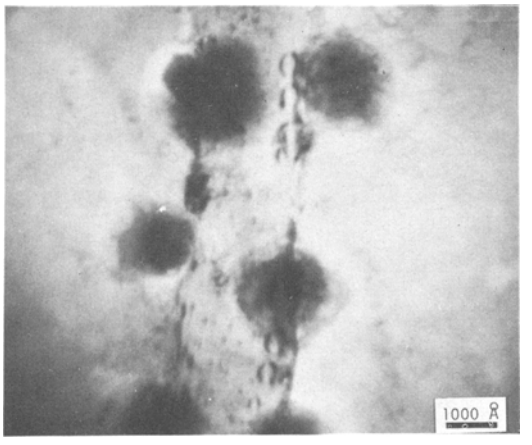

Figure 7 Electron beam stimulation of bubble nucleation in a thin foil specimen after three hours exposure to WVSA at 70° C (Alloy 1). (Note the preferential location of the hydroxide phase (pseudoboehmite) at the grain boundary/surface intersection.)

to or under pseudo-boehmite islands. It should be noted that all the bubbles formed during observation of the base alloy eventually disappeared.

3.4.2. Artificially aged

Thin foils of the artificially aged alloys showed effects due to hydrogen penetration more rapidly than the alloys in the as-quenched conditions. The preferential siting of pseudo-boehmite islands at grain-boundary/surface intersections was again observed for all the alloys. This is shown in the sequence of images in Fig. 8a, b and c for Alloy 3. The first order dark field image under weak beam conditions ($\mathbf{g} = 200$) in Fig. 8c is less useful for demonstrating bubble morphology than the weakly excited third-order bright field image ($\mathbf{g} = 600$), Fig. 8b. However, the weak beam dark field image reveals the grain-boundary dislocations (note these image widths are < 20 Å) and the presence of a more crystalline hydroxide film under the pseudo-boehmite island. These hydroxide crystallites (arrowed) are 100 to 200 Å in diameter and are either a more crystalline boehmite or possibly bayerite. Again, as with Fig. 4c under dynamical low order bright field reflecting conditions, in Fig. 8a ($\mathbf{g} = 200, s = 0$) the bubble morphology is obscured by the imaged strain fields.

Figure 8 Hydrogen bubble formation during one-hour exposure of a thin foil specimen of an artificially aged alloy (Alloy 3) to WVSA at 70° C. (a) BF $\mathbf{g} = 200, s = 0$ (b) BF $\mathbf{g} = 600, s = 0$ (c) DF $\mathbf{g}$ 200 under weak beam conditions.

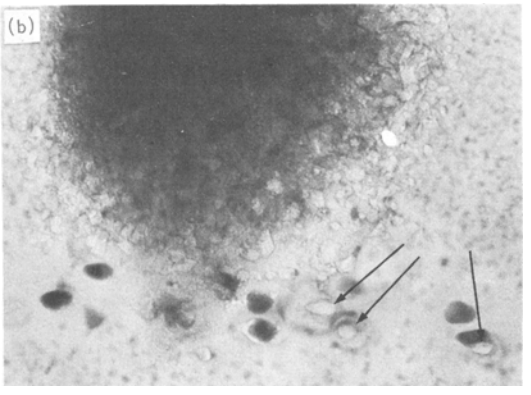

4. Discussion

Hydrogen penetration of grain boundaries in Al–Zn–Mg alloys results in a loss of grain-boundary adhesive strength and promotes intergranular embrittlement and stress-corrosion crack propagation. It is important to establish the form and morphology of the hydrogen on the boundary and with regard to this objective in the present study it has been repeatedly demonstrated that high-pressure hydrogen-filled bubbles can be formed on

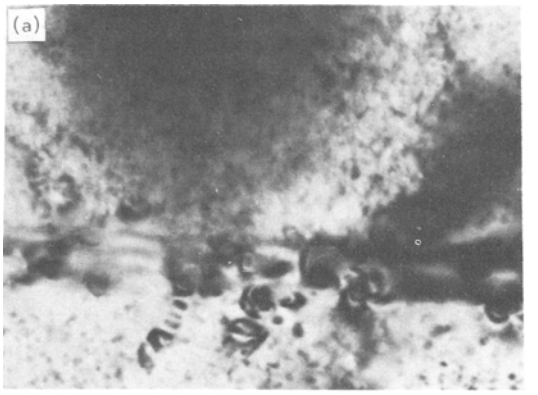

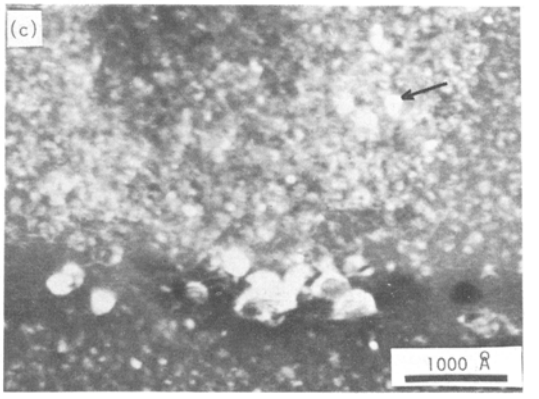

grain boundaries, particularly in aged thin foil material. However, it is probable in thicker materials that hydrogen bubbles are confined to near surface regions where a stress dilation may exist together with a higher hydrogen activity. This tendency to form bubbles when certain constraints are removed has been succinctly demonstrated when thin foils prepared from embrittled (i.e. hydrogen-containing) bulk specimens are examined under the 120 kV electron beam. The combined effect of a changed state of elastic stress constraint in the thin foil specimen and electron beam heating rapidly results in bubble formation. The molecular hydrogen within the bubble generates a significant stress as the yield stress of the surrounding matrix is soon exceeded, and dislocation generation and propagation are observed.

In bulk specimens away from surface regions it is probable therefore that even on grain boundaries where there is a high hydrogen concentration there are no bubbles. The atomic hydrogen on such boundaries is probably chemisorbed, which necessitates electronic interaction between the adsorbed hydrogen and the grain-boundary atoms. In order to form a hydrogen bubble it is necessary that the chemisorbed hydrogen be recombined to form a hydrogen molecule and desorbed. The activation barrier for this process must clearly be small as shown by the ease of bubble formation under the stimulation of a 120 kV electron beam. The chemisorbed hydrogen atom can be highly mobile and may rapidly migrate between grain-boundary sites. The precise chemical composition of the grain-boundary is therefore extremely important in determining the relative energies of adsorption and desorption and the mobility of the adsorbed hydrogen. Changes in the composition of zinc and magnesium on the grain-boundary plane, which may be controlled by the rate of quenching, can therefore be extremely significant. The role of grain-boundary precipitates is also of interest as these can effectively drain the grain-boundary plane of solute.

From the present study it has also been demonstrated that the hydrogen bubbles interact both with the grain-boundary precipitate and with intermetallic particles formed either during casting or during homogenization. In fact it has been shown that bubbles are unstable on precipitate-free boundaries. On such boundaries, for example those in rapidly quenched unaged specimens, hydrogen bubbles can be easily stimulated to develop (again by interaction with a 120 kV beam of electrons) and can subsequently readily disappear. On such boundaries which presumably have a high zinc and magnesium concentration the activation barrier for adsorption and desorption of atomic hydrogen must be extremely small. The beneficial effect on stress-corrosion resistance of additions such as chromium and possibly manganese and of various over-ageing treatments can be explained by the fact that in both cases sites are provided where stable bubbles of molecular hydrogen can be formed, perhaps in regions ahead of propagating cracks. However, the role of solute additions, apart from those which promote primary intermetallic particle formation, is complex and this study has provided no further insight into how such additions affect hydrogen accumulation and consequently intergranular embrittlement and stress-corrosion cracking. Solute additions which compete with zinc and magnesium for grain-boundary sites can obviously affect the energy required for the adsorption and desorption of hydrogen and its grain-boundary mobility or may modify the equilibrium grain-boundary precipitate.

The variation in bubble density along a single grain-boundary and from boundary to boundary supports the observation that the bubbles have an inherent crystallographic nature, i.e. a low surface energy configuration, which can best be accommodated by certain grain-boundary planes and orientations which hence provide preferential nucleation sites.

5. Conclusions

Direct high resolution observation of grain-boundaries in Al–Zn–Mg alloys with a high hydrogen concentration have shown that:

(1) In embrittled bulk specimens the hydrogen is highly mobile and in atomic form, and probably chemisorbed on the grain-boundary plane.

(2) In "thin-foil" specimens bubbles of molecular hydrogen readily form. These high pressure bubbles show affinity for both grain-boundary precipitates in overaged microstructures and for primary intermetallic phases. The formation and growth of such bubbles may locally "getter" the embrittling atomic hydrogen and render it effectively innocuous.

(3) The bubbles have the form of lenses, where the plane of the lens coincides with the grain-

boundary plane. When the bubbles are viewed in plan section they are frequently observed to be hexagonal in shape and bounded by {1 1 1} planes.

(4) Alloying additions of Fe, Si, Fe + Si, Fe + Si + Cr, Fe + Si + Mn, Fe + Si + Zr do not prevent grain-boundary hydrogen penetration.

(5) Bubble morphology is most readily discerned by using bright field imaging with a high order systematic reflection.

Acknowledgements

I am indebted to Professor P. R. Swann, Dr R. Alani and Dr. E. P. Butler of Imperial College, London for their constructive criticism of the ideas presented in this paper.

References

1. L. MONTRAIN and P. R. SWANN, Proceeding of the International Conference on Hydrogen in Metals, Seven Springs, 1973 edited by I. M. Bernstein and A. W. Thompson (A.S.M., Metals Park Ohio, 1974) p. 575.
2. G. M. SCAMANS, R. ALANI and P. R. SWANN, *Corrosion Science.* **16**, (1976), 443.
3. R. ALANI and P. R. SWANN, Imperial College, Private communication, June 1975.
4. G. M. SCAMANS and C. D. S. TUCK, Proceedings of the International Conference of Mechanisms of Environment Sensitive Cracking of Materials, Guildford 1977 edited by P. R. Swann. (to be published).
5. C. D. S. TUCK and G. M. SCAMANS, Second International Conference of Hydrogen in Metals, Paris 1977.
6. G. M. SCAMANS, Unpublished work (1975).
7. M. F. ASHBY and L. M. BROWN, *Phil Mag* 8 (1963) 1083, 1649.
8. G. W. LORIMER and R. B. NICHOLSON, *Acta Met* 14 (1966) 41.

Received 20 December 1976 and accepted 6 May 1977.